Mechanistic Study of the Deamidation Reaction of Glutamine: A Computational Approach

ARTICLE *in* THE JOURNAL OF PHYSICAL CHEMISTRY B · FEBRUARY 2014

Impact Factor: 3.3 · DOI: 10.1021/jp4107266 · Source: PubMed

3 AUTHORS:

Mohammad A Halim
French National Centre for Scientific Research
20 PUBLICATIONS **91** CITATIONS
SEE PROFILE

Mansour H. Almatarneh
University of Jordan
15 PUBLICATIONS **94** CITATIONS
SEE PROFILE

Raymond A Poirier
Memorial University of Newfoundland
140 PUBLICATIONS **2,008** CITATIONS
SEE PROFILE

THE JOURNAL OF PHYSICAL CHEMISTRY B

Article

pubs.acs.org/JPCB

Mechanistic Study of the Deamidation Reaction of Glutamine: A Computational Approach

Mohammad A. Halim,[†] Mansour H. Almatarneh,*[,‡] and Raymond A. Poirier*[,†]

[†]Department of Chemistry, Memorial University, St. John's, NL, Canada A1B 3X7

[‡]Department of Chemistry, University of Jordan, Amman 11942, Jordan

Supporting Information

ABSTRACT: Glutamine—a popular nutritional supplement, non-toxic amino acid, and an essential interorgan and intercellular ammonia transporter—can destroy the neurons' mitochondria. When glutamine enters (like a Trojan horse) into the mitochondria, in the presence of glutaminase, it reacts with water and yields glutamate and excess ammonia which opens gates in the membrane of the mitochondria and thereby destroys it. The mechanistic details underlying the molecular basis of the catabolic production of excess ammonia remain unclear. In the present paper, both 5-oxoproline-mediated and direct pathways for glutamine deamidation are studied using wave function and density functional theories. The mechanisms are studied both in the gas phase and in aqueous solution using the polarizable continuum model (PCM) and solvent model on density (SMD) solvation models. Among three glutamine deamidation pathways, a two-step pathway, GDB, shows the lowest gas phase barrier height of 189 kJ/mol with the G3MP2B3 level of theory. Incorporation of solvent through PCM and SMD models reduces the barrier height to 183 and 174 kJ/mol, respectively. For the hydrolysis of 5-oxoproline, a two-step mechanism, pathway PH-B, provides a lower gas phase energy barrier (187 kJ/mol) compared to one-step (201 kJ/mol) and three-step (227 kJ/mol) pathways at G3MP2B3. Although direct hydrolysis with OH^-, pathway DHE, has the lowest gas phase barrier of 135 kJ/mol, the solvent has little effect on the barrier. For the direct hydrolysis with OH^-/H_2O, pathway DHF, the overall barrier is 143 kJ/mol, in the gas phase at G3MP2B3. In aqueous solution, the overall barrier decreases to 76 and 75 kJ/mol with PCM and SMD, respectively, at B3LYP/6-31+G(d,p), making this the most plausible mechanism. Compared to PCM, SMD predicts lower barriers for nearly all pathways investigated.

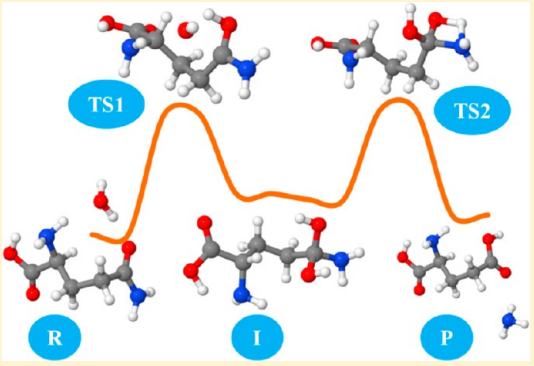

1. INTRODUCTION

Glutamine (Gln) has been viewed as a very popular, safe, and effective nutritional supplement for athletes and bodybuilders in the sports world. Because of prolonged and strenuous exercise, the body consumes Gln from both the blood plasma and the skeletal muscles.[1−6] Among all amino acids, Gln has generally been depicted metaphorically as "a Trojan horse" for its suspicious link to hyperammonemia.[7−11] This nontoxic, harmless, and neutral amino acid is mostly prevalent in blood plasma, skeletal muscles, and the central nervous system (CNS).[12−16] Interestingly, it is one of the few amino acids that can successfully cross the blood−brain barrier and its presence can be confirmed by a glutamate−glutamine cycle in the brain.[17−20] For the synthesis of nucleic acids and nucleotides, Gln acts as an important precursor and supplies the required nitrogen. It also plays a critical role in different biochemical processes, such as regulation of the acid−base balance in the kidney, urea nitrogen production, and carbon commerce for humans.[12−15]

Gln is one of the important shuttles in our system and is involved in transporting nitrogen in the form of ammonia, particularly between the different compartments of our CNS and from peripheral tissue to the kidney.[17−19,21] Since the urea cycle is not available in our CNS, the option for removing and recycling NH_3 from the brain entirely depends on Gln synthesis. NH_3 metabolism in the brain is, therefore, greatly connected with the glutamine−glutamate cycle illustrated in Figure 1.[22−26] In the presence of the astrocyte-specific enzyme (glutamine synthetase), glutamate (Glu^-) combines with ammonium ion to form Gln and H_2O in astrocytes, depicted in Scheme 1. The astrocytes' Gln is then released into the intracellular space from where it is transported into the neurons. When Gln enters into the neuron's mitochondria, in the presence of glutaminase, it reacts with H_2O and yields NH_4^+ and Glu^-. The Glu^-, which is an excitatory neurotransmitter and immediate precursor for *gamma*-aminobutyric acid (GABA), travels from the neurons to the adjacent astrocytes and completes the glutamine−glutamate cycle in the brain. Some Glu^- further reacts with H_2O in the presence of glutamate dehydrogenase and produces α-ketoglutarate

Received: October 31, 2013
Revised: February 4, 2014
Published: February 5, 2014

dx.doi.org/10.1021/jp4107266 | J. Phys. Chem. B 2014, 118, 2316−2330

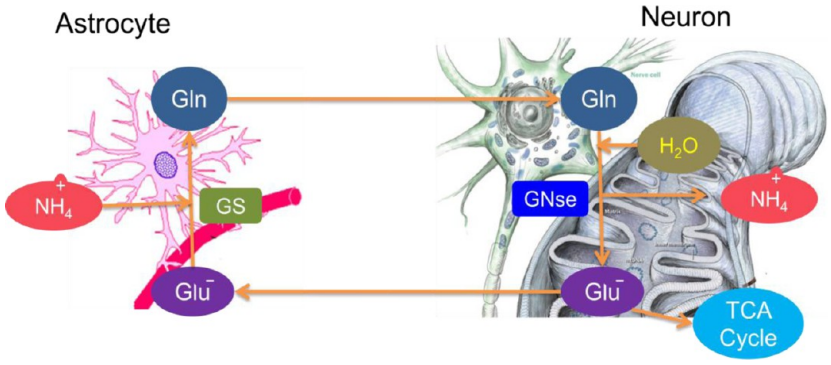

Figure 1. Glutamine (Gln)−glutamate (Glu^-) cycle in the brain. GS (glutamine synthetase), GNse (glutaminase), and TCA (tricarboxylic acid). The background image of the astrocyte is used with permission from Prof. Michelle Peckham at histology.leeds.ac.uk, and the neuron with mitochondria has been used with copyright permission from Nicolle R. Fuller of Sayo-Art.

Scheme 1. Deamidation and Amination Reactions of Glutamine and Glutamate

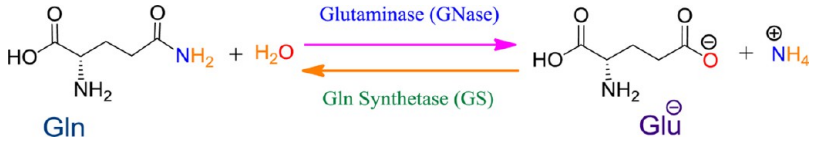

which eventually enters the tricarboxylic acid cycle (TCA) to produce energy.

Early findings by Hans Krebs and Hans Weil-Malherbe[27,28] revealed that the formation of Gln from Glu^- and NH_3 (in the presence of glutamine synthetase) is the only way NH_3 detoxification can occur in the brain (which is still prevalent in some of the literature). This dominant theme, which ignored the potential role of glutamine in neurotoxicity, was first challenged by Warren and Schenker in 1964.[29] This study disclosed that inhibiting the glutamine synthetase with methionine sulfoximine (MSO) in mice significantly increased the concentration of NH_3 in the brain; however, there were no deaths in the treated group. Therefore, they concluded that "*ammonia intoxication does not depend upon the mere presence of high cerebral ammonia levels, but is related to the so-called mechanism of detoxification by which ammonia enters into the cerebral metabolic cycles.*" However, they even focused their investigation on the entire brain, not on any particular cells such as astrocytes and neurons. Thus, this finding failed to capture the exact snapshot for Gln neurotoxicity. The role of astrocytes and neurons, more specifically the role of mitochondria in inducing NH_3 toxicity, was not disclosed in that seminal paper.

In 1979, Norenberg and Hernandez solved the structure of the glutamine synthetase enzyme in rat brain and confirmed that glutamine synthetase is exclusively present in the astrocytes, not in neurons or other cells in the brain.[30] In 1991, Hawkins and Jessy revealed that excessive amounts of NH_3 in astrocytes is less harmful before it enters into a neuron's mitochondria, and they also observed that, when NH_3 is metabolized into Gln, the toxic effect seems to commence.[31,32] In 2006, Norenberg and his coauthors first proposed the interesting "Trojan horse" hypothesis.[7] The hypothesis was based on a study performed on the phosphate-activated glutaminase responsible for deamination of glutamine in the neurons' mitochondria. After inhibiting glutaminase by DON (6-diazo-5-oxo-L-norleucine), they observed that the deamidation of Gln was slowed, which in turn reduced the formation of NH_3. Excess NH_3 in mitochondria creates two problems: (i) it creates many pores/channels/gates in the membrane of mitochondria, known as mitochondrial permeability transitions (MPTs), and (ii) it creates excessive reactive oxygen species (ROS).[33−37] Both MPT and ROS have complex connections with cell swelling and astrocyte dysfunction. Elevated NH_3 also introduces many adverse symptoms in our body including hepatic encephalopathy. In addition, when an excessive amount of NH_3 enters the brain, it creates a neurological imbalance known as hyperammonemia.[38−41] Some common symptoms of hyperammonemia include vomiting, lethargy, and slurred speech which eventually leads to cerebral edema, coma, and death.

At neutral pH, when Gln is heated at 100 °C with water, it converts to cyclic 5-oxoproline (pyrrolidone carboxylic acid) and NH_3.[42,43] The cyclic 5-oxoproline also reacts with H_2O in the presence of dilute aqueous HCl and forms glutamic acid. Interestingly, five-membered cyclic oxoproline from free Gln (without residue) is more chemically stable compared to the four-membered ring from free asparagine.[44] Because of this fact, deamidation of free Gln through the cyclic oxoproline pathway is much faster than the deamidation of free asparagine.

Deamidation of asparaginyl and glutaminyl residues—spontaneous, nonenzymatic, and physiological reactions in peptides and proteins—is a common feature in post-translational protein modifications (PTMs).[45,47−52] Deamidation plays pivotal roles in apoptosis (programmed cell death) and aging.[53−61] This reaction also contributes to some neurodegenerative diseases such as Alzheimer's, Parkinson's, and various forms of cancer, due to excessive and inappropriate apoptosis.[56] PTM of the human lens' crystallins is also a result of deamidation, and these lenses are ideal candidates for studying protein aging.[62−65] Interestingly, the half-life of the deamidation of asparagine and glutamine residues in peptides and proteins varies from one day to a century.[66] This reaction also causes time-dependent changes in the charge and conformations of peptides and proteins, and regulates protein turnover, development, and aging in a timely manner. That is why deamidation of asparagine and glutamine residues in

dx.doi.org/10.1021/jp4107266 | J. Phys. Chem. B 2014, 118, 2316−2330

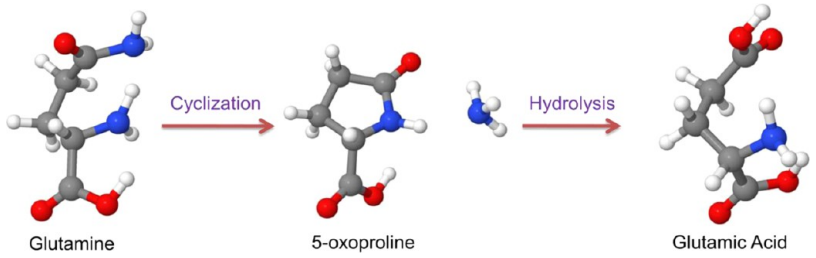

Figure 2. Deamidation of glutamine to form cyclic 5-oxoproline followed by hydrolysis. Hydrogen is white, carbon is gray, nitrogen is blue, and oxygen is red.

Table 1. Relative Enthalpies and Gibbs Energies (kJ/mol) for the Deamidation of Glutamine (GD Pathways) in the Gas Phase and in Solution at 298.15 K

	enthalpies					Gibbs energies				
structures	B3LYP/631G(d)	B3LYP/631+G(d,p)	G3MP2B3	PCM[a]	SMD[a]	B3LYP/631G(d)	B3LYP/631+G(d,p)	G3MP2B3	PCM[a]	SMD[a]
Gln Deamidation: Pathway GDA										
SR[b]	−6	−7	−4	−17	−10	−7	−7	−4	−12	−7
TS1	283	283	276	202	192	291	292	285	214	202
P1	−11	−13	−10	−8	97	−14	−17	−14	−25	107
SP[b]	22	10	16	−8	−2	−22	−33	−27	−46	−42
Gln Deamidation: Pathway GDB										
SR[b]	−24	−19	−16	−24	−14	−19	−16	−11	−18	−7
TS1	198	191	189	183	174	209	201	200	197	187
I1a	73	69	43	75	69	85	78	55	86	82
I1b	67	61	36	65	69	79	70	48	76	81
TS2	192	186	179	179	171	203	196	190	192	186
P	−8	−14	−14	36	85	−13	−23	−20	30	101
SP[b]	5	−2	4	−15	−6	−33	−42	−34	−52	−42
Gln Deamidation: Pathway GDC										
SR[b]	−6	−7	−3	−3	2	−6	−8	−3	−1	3
TS1	183	179	179	187	188	185	180	181	187	187
I1a	68	61	52	66	68	70	62	53	65	68
I1b	93	50	41	95	89	91	52	50	93	89
TS2	295	276	283	288	275	296	281	285	296	285
I2a	73	66	70	91	82	81	75	69	102	92
I2b	84	73	48	87	85	91	78	56	93	91
TS3=TS2B	209	198	192	200	187	215	204	198	209	196
P = PB	10	−2	−1	57	12	−1	−15	−12	47	−11
SP[b]	22	10	17	7	10	−21	−33	−26	−34	−31

[a]Calculated at the B3LYP/6-31+G(d,p) level of theory. [b]Separated reactants (SR) and separated products (SP).

proteins has been mentioned as a "biological timer" or "molecular clock".[66]

The deamidation reaction of glutaminyl residues is, however, a less studied reaction compared to the deamidation of asparaginyl residues, since the formation of a six-membered glutarimide intermediate from glutaminyl residues is not as energetically facile compared to the five-membered succinimide intermediate from asparaginyl residues.[67,68] That is why cyclic imide-based deamidation of glutaminyl residues is slower than the deamidation of asparaginyl residues. However, direct hydrolysis with water can also proceed with a lower activation barrier for asparaginyl residues.[69] Glutaminyl residues can also follow the direct hydrolytic pathway for deamidation, albeit slower compared to asparaginyl residues.[46] Several studies predict that the cyclic succinimide-mediated route followed by hydrolysis is the most energetically favored pathway compared to the direct hydrolysis (less studied) route.[70−79]

To our knowledge, no experimental and computational attempts have so far focused on the "Trojan horse" hypothesis to understand the mechanism of the glutamine deamidation reaction. It should be stated here that, despite some similarities, the mechanistic features of glutaminyl residues and free glutamine (without residues) are quite different. This study employs computational mechanistic approaches to locate the most energetically favored pathway in glutamine deamidation. Moreover, it focuses on how glutamine deamidation produces excess ammonia and how other factors, including solvent and reaction media, influence the reaction mechanism.

2. COMPUTATIONAL METHOD

All calculations were carried out with the Gaussian 09 software package.[80] Equilibrium geometries of reactants, transition states, intermediates, and products were fully optimized at B3LYP/6-31G(d) and B3LYP/6-31+G(d,p) in the gas phase. For comparison with the gas phase, the non-zwitterionic form of glutamine was used for the solution phase. All attempts at optimizing the zwitterionic form in the gas phase converged to the non-zwitterionic form. Our calculations reveal that in solution the zwitterionic form is more stable by 10 kJ/mol

dx.doi.org/10.1021/jp4107266 | J. Phys. Chem. B 2014, 118, 2316−2330

Table 2. Relative Enthalpies and Gibbs Energies (kJ/mol) for the Hydrolysis of 5-Oxoproline (PH Pathways) in the Gas Phase and in Solution at 298.15 K

	enthalpies					Gibbs energies				
structures	B3LYP/631G(d)	B3LYP/631+G(d,p)	G3MP2B3	PCM[a]	SMD[a]	B3LYP/631G(d)	B3LYP/631+G(d,p)	G3MP2B3	PCM[a]	SMD[a]
Hydrolysis (5-oxoproline + H_2O): Pathway PHA										
SR[b]	17	25	12	14	5	−21	−15	−26	−16	−29
TS1	186	218	201	219	203	201	229	216	239	218
P	−7	29	6	31	33	−1	33	13	44	46
SP[b]	−16	15	3	23	31	−10	19	9	36	38
Hydrolysis (5-oxoproline + H_2O): Pathway PHB										
SR[b]	22	25	20	14	9	−16	−7	−19	−15	−23
TS1	171	182	180	187	183	180	197	190	204	196
I1a	59	81	50	96	90	72	99	63	113	105
I1b	57	75	48	95	94	67	91	57	114	108
TS2	182	200	187	207	202	193	219	199	228	220
P	0	29	17	39	45	2	36	19	49	49
SP[b]	−18	14	6	21	32	−12	26	13	37	44
Hydrolysis (5-oxoproline + OH^-): Pathway PHC										
SR[b]	419	310	311	154	118	379	273	261	122	87
TS1	123	140	129	141	139	136	157	131	162	158
I1	127	144	129	145	142	138	158	129	165	160
TS2	194	215	198	218	219	209	233	201	241	240
I2a	89	107	82	94	92	101	122	82	113	109
I2b	217	207	203	192	171	220	215	196	204	184
TS3	223	242	227	243	247	229	251	224	255	260
P	64	88	84	69	64	61	88	70	74	68
SP[b]	79	100	93	74	61	75	99	79	77	64

[a]Calculated at the B3LYP/6-31+G(d,p) level of theory. [b]Separated reactants (SR) and separated products (SP).

(PCM) and 33 kJ/mol (SMD). We have investigated different pathways for the zwitterionic form, but all our attempts to locate transition states for zwitterionic glutamine in the gas phase as well as in the solution were unsuccessful. Calculations were also performed using the G3MP2B3 Gaussian-n theory for all pathways in the gas phase. By performing frequency analysis, we also confirmed that all reactants, intermediates, and products are minima with no imaginary frequencies on the potential energy surface and all transition states have a single imaginary frequency. To confirm and characterize the transition states on the potential energy surface, intrinsic reaction coordinate (IRC) analysis was employed. In order to positively confirm the reactant and product to which each transition state is connected, the last IRC structures in both directions were further optimized. All bond distances presented in this paper are from B3LYP/6-31+G(d,p) calculations. As incorporating solvent (water) is essential to mimic the real environment for glutamine deamination in mitochondria, we employed the polarizable continuum solvation model (PCM)[81−87] and solvation model based on density (SMD).[88,89] The PCM and SMD structures were optimized at the B3LYP/6-31+G(d,p) level of theory.

3. RESULTS AND DISCUSSION

Three pathways were investigated where glutamine deamidation (GD) forms cyclic 5-oxoproline and ammonia. 5-Oxoproline, also known as pyrrolidone carboxylic acid, pyroglutamic acid, and pidolic acid, can then react with H_2O (or OH^-) to form glutamic acid (or glutamate), as demonstrated in Figure 2. A concerted single-step (GDA), a two-step (GDB), and a three-step (GDC) pathway for oxoproline formation were investigated. The three cyclization pathways were studied in only a neutral medium, as the basic medium was reported by Konuklar et al.[73] to have a high barrier, 418 kJ/mol at B3LYP/6-31G(d). For the subsequent hydrolysis of 5-oxoproline with water, two pathways, a single (PHA) and a two-step (PHB) mechanism, were explored. In addition, for the hydrolysis of oxoproline with hydroxide, a three-step (PHC) mechanism was investigated. Since no experimental or computational studies are available for deamidation of glutamine, results reported here are compared with deamidation of model asparaginyl residues as well as with sodium-bound asparagine.[56,69,73,75] Relative enthalpies of activation and Gibbs energies of activation for all pathways in the gas phase and in solution are presented in Tables 1−3.

3.1. Pathway GDA: Mechanistic and Energetic Details for Glutamine Deamidation (GD). In the single-step concerted mechanism (Figure 3), one proton from the amino nitrogen is transferred to the amido nitrogen to form the transition state GDA-TS1. In this transition state, the breaking N−H (amino) bond distance is 1.68 Å and the forming N−H (amido) bond length is 1.08 Å, indicating a late transition state. In addition, the amino nitrogen simultaneously attacks the carbonyl carbon (cyclization), with a C−N bond distance of 2.25 Å, to form a five-membered ring GDA-P. In GDA-TS1, the C−N bond (1.58 Å) with the amido group is slightly longer than the C−N bond (1.47 Å) in glutamine. In this concerted mechanism, both proton transfer and cyclization occur synchronously, which is also a common feature in the concerted deamidation mechanism of asparagine residue.[69] On the basis of IRC calculations, GDA-TS1 connects with the reactant glutamine and with a complex of oxoproline and NH_3, denoted as GDA-P.

In solution, the geometry of GDA-TS1 changes significantly. The C−N bond is shortened from 2.25 Å (gas phase) to 1.66 Å with PCM and 1.61 Å with SMD, as illustrated in Figure S1

dx.doi.org/10.1021/jp4107266 | J. Phys. Chem. B 2014, 118, 2316−2330

Table 3. Relative Enthalpies and Gibbs Energies (kJ/mol) for all Direct Hydrolysis (DH) Pathways in the Gas Phase and in Solution at 298.15 K

	enthalpies					Gibbs energies				
structures	B3LYP/ 6-31G(d)	B3LYP/ 6-31+G(d,p)	G3MP2B3	PCM[a]	SMD[a]	B3LYP/ 6-31G(d)	B3LYP/ 6-31+G(d,p)	G3MP2B3	PCM[a]	SMD[a]
(Gln + H_2O): Pathway DHA										
SR[b]	20	8	14	8	5	−20	−32	−25	−29	−27
TS1	167	180	187	174	171	180	193	201	189	182
P	4	−6	15	28	30	−5	−8	7	−9	32
SP[b]	8	15	21	26	39	−30	−23	−17	−11	5
(Gln + H_2O): Pathway DHB										
SR[b]	43	32	32	19	14	3	−8	−8	−20	−16
TS1	195	195	197	191	189	207	208	209	203	206
I1a	87	92	67	95	88	95	100	76	103	104
I1b	77	84	58	89	86	88	97	69	99	102
TS2	204	215	204	204	195	216	228	216	213	213
P	27	17	33	39	103	19	14	24	−1	116
SP[b]	31	38	39	37	48	−7	1	1	−2	16
(Gln Tautomer + H_2O): Pathway DHC										
SR[b]	49	191	34	4	−5	9	153	−5	−42	−52
TS1	161	166	180	121	98	173	176	193	115	100
I1a	−16	−2	−12	−26	−22	−7	5	−3	−32	−30
I1b = I1bB	−26	−10	−21	−6	−2	−15	2	−11	−3	−2
TS2=TS2B	102	120	125	109	107	113	133	137	110	108
P	−76	−77	−47	−56	16	−85	−81	−55	−103	12
SP[b]	−71	−56	−41	−57	−40	−110	−95	−79	−104	−88
(Gln + OH^-): Pathway DHD										
SR[b]	405	245	281	33	14	365	202	241	4	−20
TS1	133	102	125	64	77	144	110	136	81	87
I1a	136	105	123	59	59	144	110	132	74	71
I1b	155	124	137	68	66	165	130	147	85	74
TS2	213	180	205	138	166	220	184	212	151	171
P	−6	−20	12	−66	−48	−14	−34	5	−69	−60
SP[b]	−10	−40	−7	−95	−67	−47	−80	−44	−123	−99
(Gln + OH^-): Pathway DHE										
SR[b]	261	153	160	−20	−53	216	108	116	−60	−90
TS1	92	94	81	97	98	97	99	86	103	104
I1	90	92	71	88	87	93	95	74	91	92
TS2	141	152	135	144	136	145	156	139	150	144
I2a	4	24	10	9	−5	9	28	15	14	−3
I2b=I1bD	11	32	16	15	−2	16	37	22	20	4
TS3=TS2D	69	87	84	85	98	71	90	87	86	101
P=PD	−151	−112	−109	−118	−115	−162	−127	−121	−134	−130
SP[b]	−154	−132	−128	−148	−135	−196	−173	−170	−187	−169
(Gln + OH^-/H_2O): Pathway DHF										
SR[b]	429	295	294	47	24	351	223	216	−19	−43
TS1	93	99	88	53	71	103	111	99	65	84
I1a	80	92	72	37	48	90	104	80	50	60
I1b	112	125	105	56	55	123	139	116	71	74
TS2	132	146	143	76	75	146	167	157	99	98
P	−42	−20	−32	−83	−52	−47	−19	−38	−88	−59
SP[b]	14	10	5	−81	−58	−61	−59	−70	−145	−122

[a]Calculated at the B3LYP/6-31+G(d,p) level of theory. [b]Separated reactants (SR) and separated products (SP).

(Supporting Information). The N−H (amido) bond distance increases from 1.08 Å in the gas phase to 1.29 and 1.30 Å while the N−H (amino) bond distance decreases from 1.68 Å in the gas phase to 1.31 and 1.30 Å for PCM and SMD, respectively. With both solvation models, the C−N (amido) bond distance remains nearly unchanged.

For the GDA pathway, the gas phase enthalpy of activation is 283 kJ/mol at both B3LYP/6-31G(d) and B3LYP/6-31+G(d,p) and 276 kJ/mol at G3MP2B3; see Table 1. For a model peptide of L-asparaginyl residues, the calculated gas phase activation barrier of the concerted mechanism is 246 kJ/mol lower than that for glutamine.[69] The production of cyclic succinimide from the asparaginyl residues is quite different. For cyclic succinimide, proton transfer occurs between one amido nitrogen containing a methyl substituent to the other amido nitrogen in asparaginyl residues,[75] whereas in glutamine the

dx.doi.org/10.1021/jp4107266 | J. Phys. Chem. B 2014, 118, 2316−2330

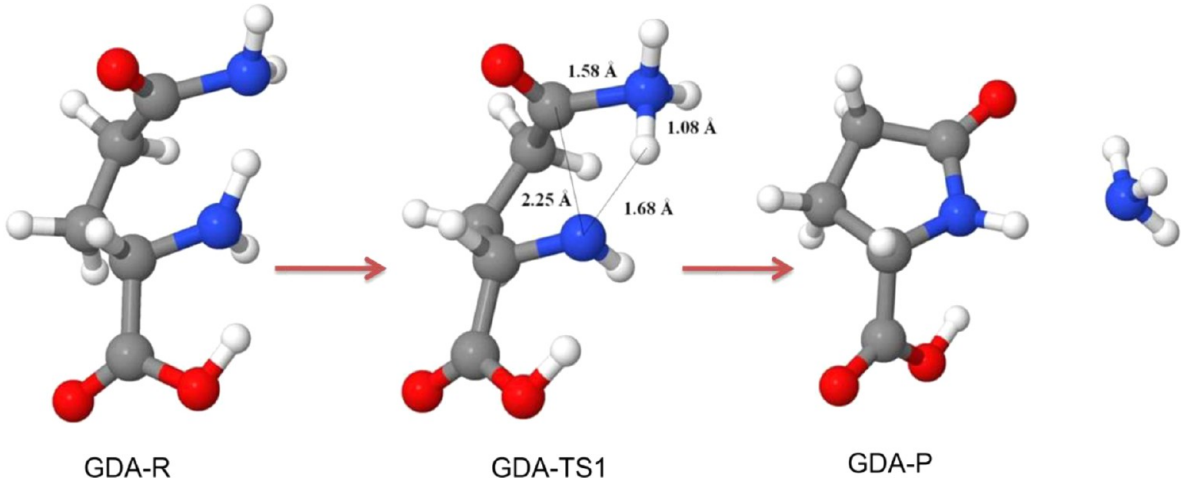

Figure 3. Pathway GDA: Deamidation of glutamine to form cyclic oxoproline and ammonia through a single-step mechanism, where optimized structures are generated at B3LYP/6-31+G(d,p) in the gas phase.

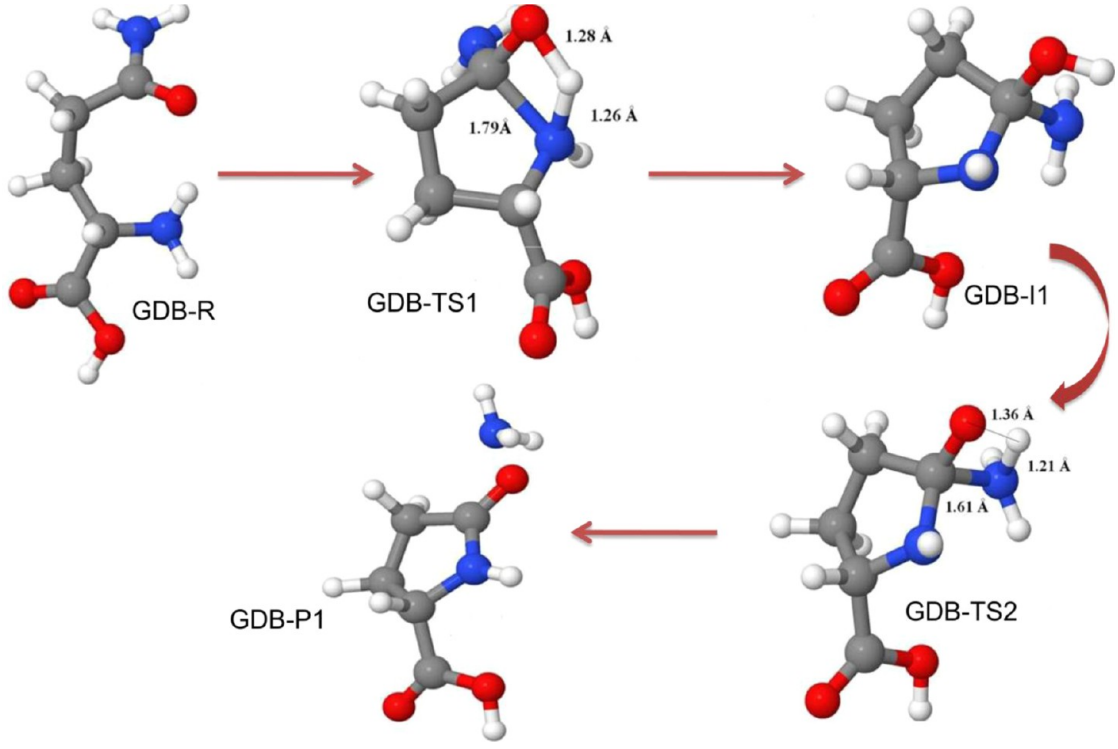

Figure 4. Pathway GDB: Deamidation of glutamine to form cyclic oxoproline and ammonia through a two-step mechanism, where optimized structures are generated at B3LYP/6-31+G(d,p).

proton migrates from the amino group to the amido group. In going from gas phase to aqueous solution, the activation barrier decreases significantly, by 81 kJ/mol (PCM) and 91 kJ/mol (SMD) at B3LYP/6-31+G(d,p). This lowering of the barrier height is also consistent with the significant changes found in the transition structure, GDA-TS1. The lowest barrier height, 192 kJ/mol, is observed with SMD which is significantly higher than the barrier (167 kJ/mol) observed for a model peptide asparaginyl residue with PCM.[75] The reason for the lower barrier for the asparaginyl residues may be due to the vicinity of the residual group present in the asparaginyl system, whereas no such group is present in free glutamine.

3.2. Pathway GDB: Mechanistic and Energetic Details for Glutamine Deamidation. The two-step pathway, GDB, proceeds through the first transition state, GDB-TS1, where one proton transfers from the amino nitrogen to the carbonyl oxygen, whereas, for the GDA pathway, one proton transfers from the amino nitrogen to the amido nitrogen. In GDB-TS1, the amino N−H bond (1.26 Å) is cleaved whereas the O−H bond (1.28 Å) is formed, as shown in Figure 4. The carbonyl carbon amino nitrogen C−N bond (cyclization) is already formed in GDB-TS1 with a bond distance of 1.79 Å, much shorter than the distance (2.25 Å) observed in GDA-TS1. IRC calculations connect the first transition state (GDB-TS1) with glutamine and with a five-membered cyclic tetrahedral intermediate, GDB-I1a. In the second transition state, GDB-TS2, one proton is almost completely transferred from the oxygen to the nitrogen through a 1,3-proton shift to form a

dx.doi.org/10.1021/jp4107266 | J. Phys. Chem. B 2014, 118, 2316−2330

complex of 5-oxoproline and NH_3, GDB-P. In GDB-TS2, the O−H bond distance is 1.36 Å, whereas the N−H bond length is 1.21 Å. A slight lengthening of the amido C−N bond (1.61 Å) is observed relative to the C−N bond distance of intermediate GDB-I1a.

When solvent effects are included, the C−N distance of GDB-TS1 decreases from 1.79 Å in the gas phase to 1.62 Å (PCM) and 1.58 Å (SMD). However, a small change appears for N−H and O−H bond distances in GDB-TS1. The C−N bond distance of GDB-TS2 decreases 1.61 to 1.56 Å with both PCM and SMD.

The overall activation barrier for this two-step mechanism is lower than that for the single-step concerted GDA pathway. At G3MP2B3, the barrier height is 189 kJ/mol. As illustrated in Figure 5 and Table 1, the barrier heights (GDB-TS1) calculated

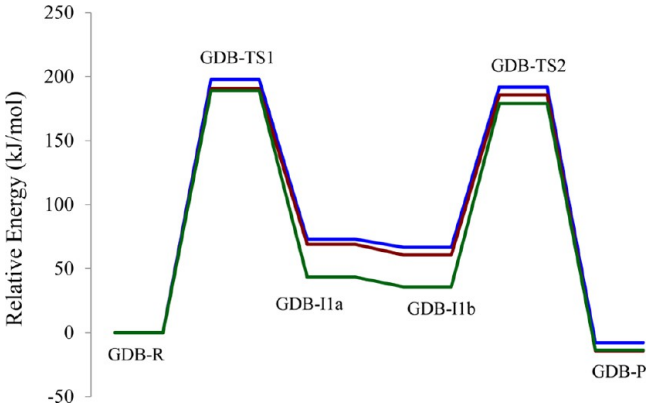

Figure 5. Pathway GDB: Gas phase relative enthalpies (kJ/mol) at B3LYP/6-31G(d) (blue), B3LYP/6-31+G(d) (red), and G3MP2B3 (green).

at B3LYP/6-31G(d) and B3LYP/6-31+G(d,p) are higher by 9 and 2 kJ/mol, respectively, compared to G3MP2B3. In this two-step mechanism, the first step (GDB-TS1) is the rate-determining step at all levels of theory. However, for the deamidation of asparaginyl residues, the second step is the rate-determining step with a barrier height of 211 kJ/mol at B3LYP/6-31+G(d,p)[69] compared to 191 kJ/mol for the GDB pathway. GDB-TS1 and GDB-TS2 are connected by two intermediates, GDB-I1a and GDB-I1b. These cyclic intermediates differ in the conformation of the amino hydrogen and hydroxyl groups. These conformational changes are reported for the deamination of cytosine, guanine, and adenine.[90−94] Since these conformers differ by no more than 10 kJ/mol at all levels of theory, only the more stable structure will be reported in the figures. GDB-TS2 is slightly lower than GDB-TS1 by 6, 5, and 10 kJ/mol at B3LYP/6-31G(d), B3LYP/6-31+G(d,p), and G3MP2B3, respectively, as shown in Table 1 and Figure 5.

For the GDB pathway, the solvent produces only small changes to the geometry of the transition structure with a corresponding slight decrease in the barrier for the first step (GDB-TS1), 8 and 17 kJ/mol for PCM and SMD, respectively (Figure S2, Supporting Information).

3.3. Pathway GDC: Mechanistic and Energetic Details for Glutamine Deamidation. In contrast to the single-step and two-step pathways, in the GDC pathway, the first step is conversion of glutamine to its tautomeric form (GDC-I1a) by transferring one proton from the amido nitrogen to the carbonyl oxygen via GDC-TS1, illustrated in Figure S3 (Supporting Information). This mechanism is comparable to the three-step mechanism for succinimide formation from asparagine residues, where step 1 proceeds through a side-chain tautomerization.[69] In GDC-TS1, the N−H (breaking) and O−H (forming) bond lengths are nearly the same (1.33 and 1.31 Å). For step 2 (GDC-TS2), one proton transfers from the amino nitrogen to the amido nitrogen and simultaneously the amino nitrogen attacks the carbonyl carbon to form the five-membered ring. The forming N−C bond distances in GDC-TS2 (2.26 Å) and GDA-TS1 (2.25 Å) are nearly the same but quite longer than the C−N bond distance in GDB-TS1 (1.79 Å). GDC-TS2 is connected to intermediates GDC-I1b and GDC-I2a. In the final step, the reaction proceeds via GDB-TS2, converting intermediate GDC-I2b into the final product, where GDC-I2a and GDC-I2b differ only in conformation.

Solvent has very little effect on the first step (GDC-TS1) with no noticeable changes in the geometry of the transition state. For the second step (GDC-TS2), both PCM and SMD, however, favor the N−H (amido) bond cleavage by lengthening the bond from 1.18 Å (gas phase) to 1.47 Å (PCM) and 1.46 Å (SMD). PCM and SMD also significantly decrease the C−N bond distance, from 2.26 Å in the gas phase to 1.62 Å with PCM and 1.59 Å with SMD.

The barrier associated with the first transition state (GDC-TS1) is 183, 179, and 179 kJ/mol at B3LYP/6-31G(d), B3LYP/6-31+G(d,p), and G3MP2B3, respectively. These results indicate that the gas phase tautomerization barrier for glutamine is very close to the asparagine residues barrier of 186 kJ/mol at B3LYP/6-31+G(d,p).[69] The second step of the GDC pathway is the rate-determining step, resulting in an overall barrier of 295, 276, and 283 kJ/mol at B3LYP/6-31G(d), B3LYP/6-31+G(d,p), and G3MP2B3, respectively (shown in Figure S4, Supporting Information, and Table 1). This is expected, since GDB-TS2, which involves a 1,3-proton shift of the hydroxyl hydrogen to the amino group to yield a complex of 5-oxoproline and NH_3, is product-like (late TS), whereas GDC-TS2 is an early TS and involves formation of a C−N bond (2.26 Å) to form a five-membered ring (the cyclic oxoproline). A three-step mechanism for the deamidation of the asparaginyl residues has a lower barrier, 211 kJ/mol at B3LYP/6-31+G(d,p).[69] The overall barrier for the three-step cyclic GDC pathway is higher by 6 kJ/mol than that for pathway GDA and by 94 kJ/mol for pathway GDB.

In aqueous solution, the barrier height for the first step (GDC-TS1) only increases by 8 kJ/mol (PCM) and 9 kJ/mol (SMD), as shown in Figure S5 (Supporting Information). For the second step (GDC-TS2), PCM also increases the barrier by 12 kJ/mol, while SMD lowers the barrier by only 1 kJ/mol compared to the gas phase.

Among three possible routes for cyclization, the two-step mechanism of pathway GDB is the most energetically favored route with an overall barrier of 189 kJ/mol in the gas phase at the G3MP2B3 level of theory. The experimental study of the deamidation reaction of sodium-bound asparagine[56] predicts a lower activation barrier, 155 kJ/mol. In the gas phase, a lower barrier, 168 kJ/mol, is also obtained for sodium-bound asparagine with B3LYP/6-311+G(2d,2p). For pathway GDB, the computed barrier is reduced to 174 kJ/mol in aqueous solvent with SMD.

3.4. Pathway PHA: Mechanistic and Energetic Details for the Hydrolysis of Cyclic 5-Oxoproline with Water. In this single-step concerted mechanism, 5-oxoproline reacts with water to yield glutamic acid. This hydrolysis reaction occurs when one proton from the water migrates to the nitrogen of

dx.doi.org/10.1021/jp4107266 | J. Phys. Chem. B 2014, 118, 2316−2330

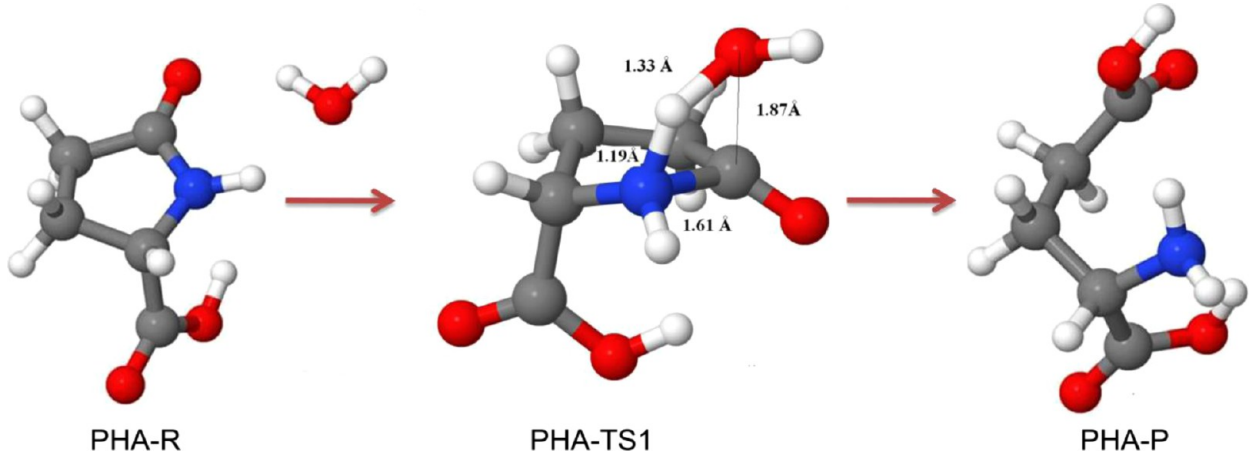

Figure 6. Pathway PHA: Hydrolysis of cyclic 5-oxoproline with water through a single-step mechanism, where optimized structures are generated at B3LYP/6-31+G(d,p).

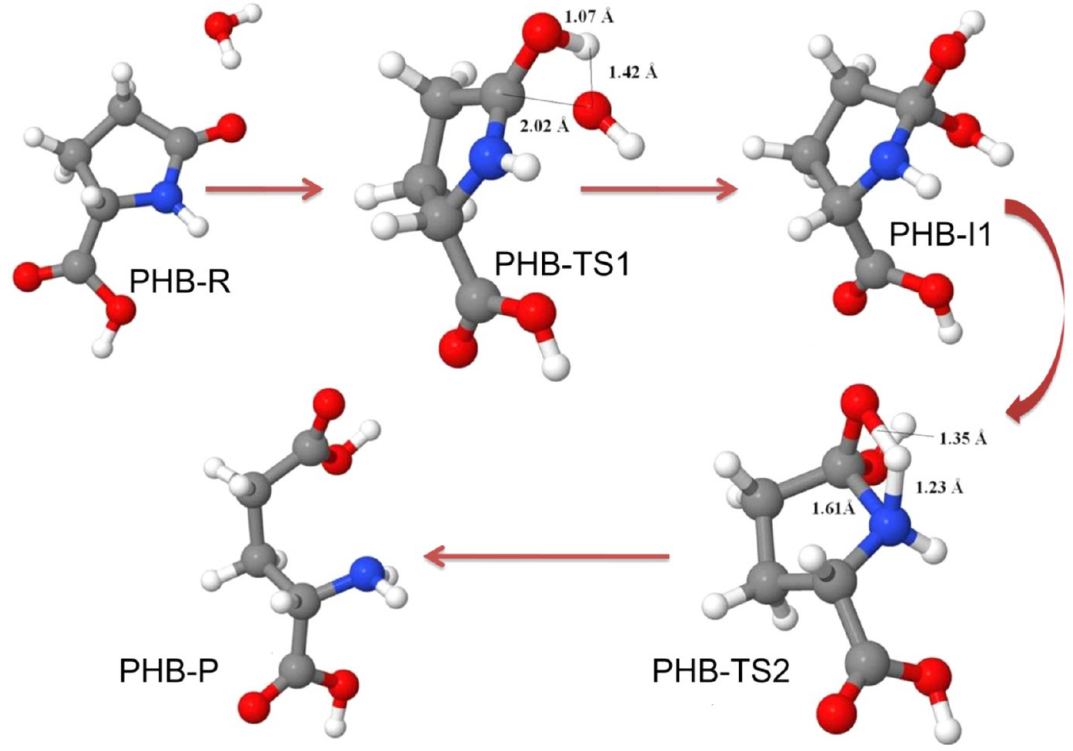

Figure 7. Pathway PHB: Hydrolysis of cyclic 5-oxoproline with water through a two-step mechanism, where optimized structures are generated at B3LYP/6-31+G(d,p).

oxoproline and the oxygen of the water simultaneously attacks the electron deficient carbonyl carbon, PHA-TS1. In the transition structure, the O−H bond (1.33 Å) is almost broken and the N−H bond (1.19 Å) is almost completely formed, while the O−C bond (1.87 Å) is still fairly long, as depicted in Figure 6. Ring-opening occurs synchronously, where the C−N bond lengthens from 1.47 Å in oxoproline to 1.61 Å in PHA-TS1 to yield glutamic acid, PHA-P.

Solvation promotes the O−H bond cleavage which increases from 1.33 Å in the gas phase to 1.45 Å with PCM and 1.67 Å with SMD. Solvent also promotes N−H bond formation by shortening the distance from 1.19 Å in the gas phase to 1.12 Å with PCM and 1.06 Å with SMD. Compared to PCM, the changes in bonding are more pronounced with SMD. Solvent, however, causes a slight shortening of the C−N bond, associated with ring-opening, from 1.61 to 1.59 Å with PCM and 1.55 Å with SMD. The nucleophilic addition of water to the carbonyl carbon is also affected by solvent, as revealed by a noticeable lengthening of the C−O bond to 2.01 Å (PCM) and 2.18 Å (SMD) compared to the gas phase (1.87 Å).

The gas phase activation barrier associated with the transition state PHA-TS1 is 186, 218, and 201 kJ/mol calculated at B3LYP/6-31G(d), B3LYP/6-31+G(d,p), and G3MP2B3, respectively. The gas phase B3LYP/6-31G(d) barrier height (186 kJ/mol) is in good agreement with the G3MP2B3 value (201 kJ/mol), both lower than the B3LYP/6-31+G(d,p) barrier (218 kJ/mol) and lower than the calculated barrier of 244 kJ/mol for the asparaginyl residues.[69] SMD decreases the barrier height to 203 kJ/mol, while PCM has little effect.

dx.doi.org/10.1021/jp4107266 | J. Phys. Chem. B 2014, 118, 2316−2330

3.5. Pathway PHB: Mechanistic and Energetic Details for the Hydrolysis of Cyclic 5-Oxoproline with Water. The two-step hydrolysis pathway, PHB, proceeds when a complex of oxoproline and water, PHB-R, undergoes a proton transfer from the water to the carbonyl oxygen and the oxygen of the water attacks the carbonyl carbon to form a four-center transition structure, PHB-TS1. As seen in Figure 7, the O−H bond of the water is 1.42 Å (breaking) and the two bonds being formed, the O−H bond of the carbonyl and the O−C bond, are 1.07 and 2.02 Å, respectively. PHB-TS1 and PHB-TS2 are connected by two tetrahedral intermediates, PHB-I1a and PHB-I1b, which differ only in their conformation. The last step, PHB-TS2, is a 1,3-proton shift leading to glutamic acid, PHB-P.

In solution, the proton transfer from the water to the carbonyl oxygen (PHB-TS1) is much more advanced. The O−H (water) bond length with PCM and SMD is 1.56 and 1.90 Å, respectively, compared to 1.42 Å in the gas phase. The nucleophilic addition of water to the carbonyl carbon is, however, not as advanced in aqueous solution, where the C−O bond distance increases from 2.02 Å (gas phase) to 2.09 Å (PCM) and 2.24 Å (SMD). In the second transition structure (PHB-TS2), ring-opening (C−N bond) is not as advanced in aqueous solution, 1.57 and 1.55 Å with PCM and SMD, respectively; compare to 1.61 Å in the gas phase.

For the first step, the gas phase B3LYP/6-31+G(d,p) barrier (182 kJ/mol) is in good agreement with the G3MP2B3 barrier (180 kJ/mol) compared to 171 kJ/mol at B3LYP/6-31G(d). As illustrated in Figure 8, the second step is the rate-determining

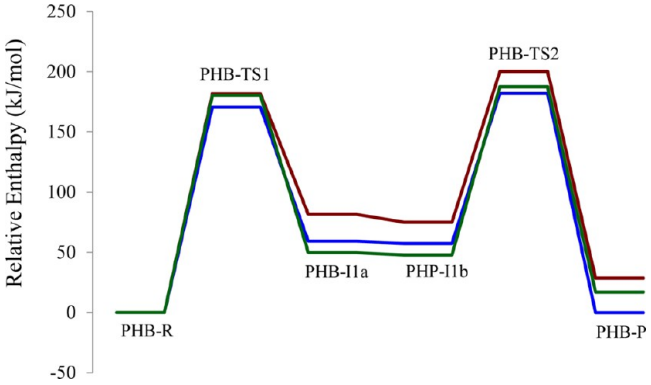

Figure 8. Pathway PHB: Gas phase relative enthalpies (kJ/mol) at B3LYP/6-31G(d) (blue), B3LYP/6-31+G(d) (red), and G3MP2B3 (green).

step at all levels of theory with an overall activation energy of 182, 200, and 187 kJ/mol at B3LYP/6-31G(d), B3LYP/6-31+G(d,p) and G3MP2B3, respectively, given in Table 2. The B3LYP/6-31+G(d,p) barrier, 200 kJ/mol, is 26 kJ/mol lower than the barrier for the asparaginyl residue.[69] PCM and SMD have very little effect on PHB-TS1 or PHB-TS2, as depicted in Figure S6 (Supporting Information).

3.6. Pathway PHC: Mechanistic and Energetic Details for the Hydrolysis of Cyclic 5-Oxoproline with OH^-. In the presence of hydroxide, 5-oxoproline is deprotonated to form a complex of the oxoproline anion and water (PHC-R). The hydrolysis of 5-oxoproline anion with water follows a three-step mechanism that leads to glutamate (PHC-P). This first step is a nucleophilic addition with simultaneous hydrogen transfer back to the carboxylic group to form intermediate PHC-I1. The forming C−O bond in PHC-TS1 is 1.74 Å, as illustrated in Figure S7 (Supporting Information). The second step is a concerted proton transfer from the hydroxyl group to the neighboring carbonyl oxygen. In step three, PHC-TS3, a 1,3-proton shift from the OH group to the amino nitrogen, occurs along with ring-opening where the C−N bond lengthens to 2.21 Å. IRC calculations revealed two different intermediates, PHC-I2a (from TS2) and PHC-I2b (from TS3), which is significantly higher in energy (Figure S8, Supporting Information). The intermediates differ in the position of the hydroxyl groups and conformation of the N−H (Figure S7, Supporting Information). In spite of extensive attempts, we were not successful in connecting these two intermediates. We were also unsuccessful at connecting PHC-I2a to an alternative TS3. Since the overall barrier for this pathway is quite high, this does not change any of the conclusions.

Both PCM and SMD predict little change in PHC-TS1 or PHC-TS2. Solvent, however, enhances ring-opening, where PCM and SMD elongate the C−N bond distance by 0.12 and 0.24 Å, respectively, from 2.21 Å in the gas phase. With SMD, the elongation of the C−N bond significantly disfavors the 1,3-proton transfer from the OH group to the amino nitrogen by increasing the N−H bond distance from 2.02 Å in the gas phase to 3.12 Å.

In the gas phase, as given in Table 2 and seen in Figure S8 (Supporting Information), the first step has the lowest barrier at all levels of theory, 123 kJ/mol at B3LYP/6-31G(d), 140 kJ/mol at B3LYP/6-31+G(d,p), and 129 kJ/mol at G3MP2B3. The tetrahedral intermediate, PHC-I1, is very close in energy to PHC-TS1. The energy of the second transition state, PHC-TS2, is significantly higher, 215 kJ/mol at B3LYP/6-31+G(d,p) and 198 kJ/mol at G3MP2B3. The second intermediate, PHC-I2a, is considerably more stable than PHC-I1 and PHC-I2b. The third step is predicted to be the rate-determining step at all levels of theory. The overall activation barrier for this pathway is 223, 242, and 227 kJ/mol with B3LYP/6-31G(d), B3LYP/6-31+G(d,p), and G3MP2B3, respectively, as depicted in Figure S8 (Supporting Information) and given in Table 2. Inclusion of aqueous solvent, with both PCM and SMD, only slightly increases the overall barrier (no more than 5 kJ/mol), as illustrated in Figure S9 (Supporting Information).

For hydrolysis of cyclic 5-oxoproline with water through the two-step mechanism, pathway PHB exhibits the lowest overall activation barrier, 187 kJ/mol, in the gas phase at G3MP2B3 and 202 kJ/mol in the condensed phase with SMD.

4. MECHANISTIC DETAILS OF DIRECT HYDROLYSIS PATHWAYS (DH)

In addition to the GD and PH mechanisms, glutamine can undergo deamidation through direct hydrolysis (DH) pathways in which glutamine reacts with water (as well as with hydroxide and a hydronium ion) to produce glutamic acid and ammonia, as depicted in Figure 9. A previous experimental study showed that glutaminyl residues can also undergo deamidation through a direct hydrolytic pathway.[46] Although no mechanism for the deamidation of free glutamine has been reported in the literature, direct hydrolysis has been reported for other similar systems. These reactions, including deamination of formamidine, cytosine, adenine, guanine, and 8-oxoguanine with H_2O, OH^-, and OH^-/H_2O, indicate that direct hydrolysis can significantly lower the barrier height through a network of hydrogen bonds in the transition state.[90−100] A recent finding reveals that direct hydrolysis with water can also proceed with a lower activation barrier for asparaginyl residues.[69] In this study,

dx.doi.org/10.1021/jp4107266 | J. Phys. Chem. B 2014, 118, 2316−2330

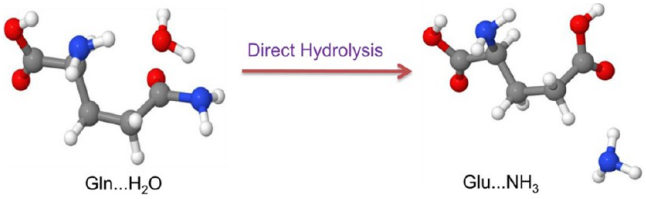

Figure 9. Direct hydrolysis of glutamine with water (as well as hydronium ion and hydroxide) yields glutamic acid (Glu) and ammonia.

six pathways for direct hydrolysis of free glutamine with concerted and stepwise mechanisms were considered.

4.1. Pathway DHA: Mechanistic and Energetic Details of Direct Hydrolysis with Water. In a single-step concerted mechanism, one proton from the water molecule transfers to the nitrogen of the amido group, while the oxygen of the water molecule approaches the carbonyl carbon, illustrated in Figure 10. DHA-TS1 is a four-center transition state analogous to that found in the study of the deamidation of asparaginyl residues.[69] In DHA-TS1, a proton is already transferred from the water molecule to the amido sp^2 nitrogen atom (N−H distance 1.09 Å) with substantial lengthening of the C−N bond (1.61 Å), indicating a late transition state but the oxygen of the water molecule is still relatively far (the O−C distance is 1.99 Å). This single step pathway yields a complex of glutamic acid and ammonia, DHA-P.

Aqueous solvent results in a substantial lengthening of the O−H bond, from 1.53 Å in the gas phase to 1.70 Å with PCM and 1.84 Å with SMD. In addition, the gas phase N−H bond distance (1.09 Å) is shortened accordingly to 1.06 Å (PCM) and 1.04 Å (SMD). In solution, however, the nucleophilic addition is not as advanced. With both PCM and SMD, the C−O bond distance increases by 0.13 and 0.20 Å, respectively, from 1.99 Å in the gas phase. A corresponding decrease of the C−N bond also occurs, from 1.61 to 1.56 and 1.53 Å with PCM and SMD, respectively, which implies an earlier transition state with respect to elimination of NH_3.

For pathway DHA, the activation energy at B3LYP/6-31G(d), B3LYP/6-31+G(d,p), and G3MP2B3 is 167, 180, and 187 kJ/mol, respectively. The B3LYP/6-31+G(d,p) barrier height is 180 kJ/mol compared to 200 kJ/mol for the direct hydrolysis of the asparaginyl residue with one water molecule.[69] In addition, barriers for the mechanism based on succinimide formation with concerted and tautomerization pathways are also 66 and 31 kJ/mol higher than those for pathway DHA at B3LYP/6-31+G(d,p).[69] A similar study on the deamination reaction of adenine with a single water molecule gives a higher barrier (247, at B3LYP/6-31G(d,p)) for the rate-determining step.[96] The previous study on the deamination reaction of formamidine and cytosine with one water molecule also gives a high barrier for the rate-determining step of 213 (at G2) and 221 kJ/mol (at G3MP2), respectively.[95,90] PCM reduces the gas phase barrier by 6 kJ/mol and SMD lowers the barrier by 9 kJ/mol at B3LYP/6-31+G(d,p).

4.2. Pathway DHB: Mechanistic and Energetic Details of Direct Hydrolysis with Water. As shown in Figure S10 (Supporting Information), for this two-step mechanism, in the first step, a proton from the water transfers to the carbonyl oxygen. The H_2O oxygen is relatively far from the carbonyl carbon (O−C distance 2.08 Å) in DHB-TS1. The DHB-TS1 transition state leads to a tetrahedral intermediate, DHB-I1a, which connects to the second transition state (DHB-TS2) via DHB-I1b. In DHB-TS2, one proton shifts from the hydroxyl group to the nitrogen of the amido group, where the O−H and N−H bond distances are 1.36 and 1.22 Å, respectively, and the C−N bond distance is 1.60 Å, as presented in Figure S10 (Supporting Information). The internal proton transfer results in the deamidation product, a complex of glutamic acid and NH_3, DHB-P.

Similar to the DHA-TS1 transition state, aqueous solvent also promotes the proton transfer from the water molecule to the carbonyl oxygen in DHB-TS1. PCM and SMD increase the O−H (water) bond distance by 0.10 and 0.32 Å, respectively, from the gas phase distance of 1.49 Å. The corresponding O−H bond distance (carbonyl oxygen) is decreased by 0.03 and 0.06 Å with PCM and SMD, respectively. The nucleophilic attack to the carbonyl carbon, on the other hand, is less advanced where, with PCM and SMD, the C−O bond distance is increased from 2.08 to 2.13 and 2.23 Å, respectively.

All levels of theory predict the barrier for the first step of the DHB pathway to be higher than that for the DHA pathway. The barrier is higher by 28, 15, and 10 kJ/mol at B3LYP/6-

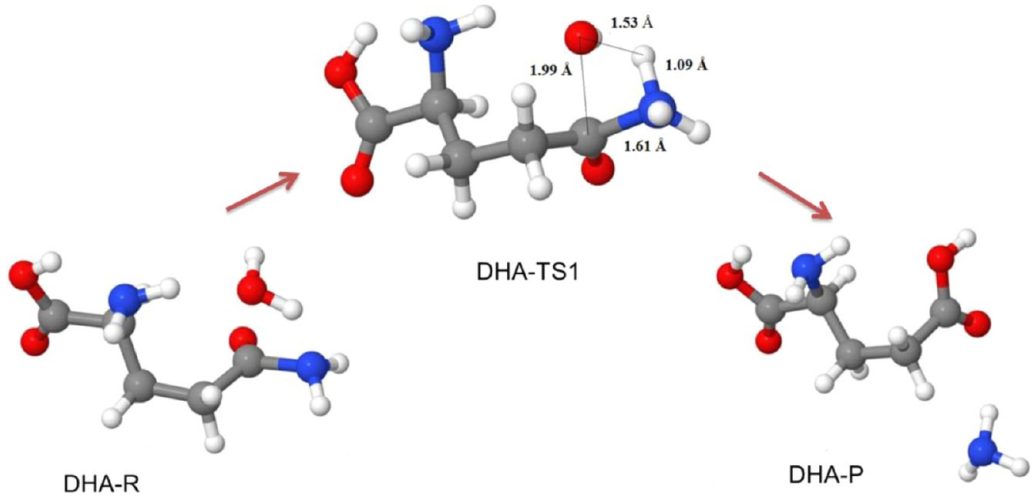

Figure 10. Pathway DHA: Direct hydrolysis of glutamine with a water through a single-step mechanism, where optimized structures are generated at B3LYP/6-31+G(d,p).

dx.doi.org/10.1021/jp4107266 | J. Phys. Chem. B 2014, 118, 2316−2330

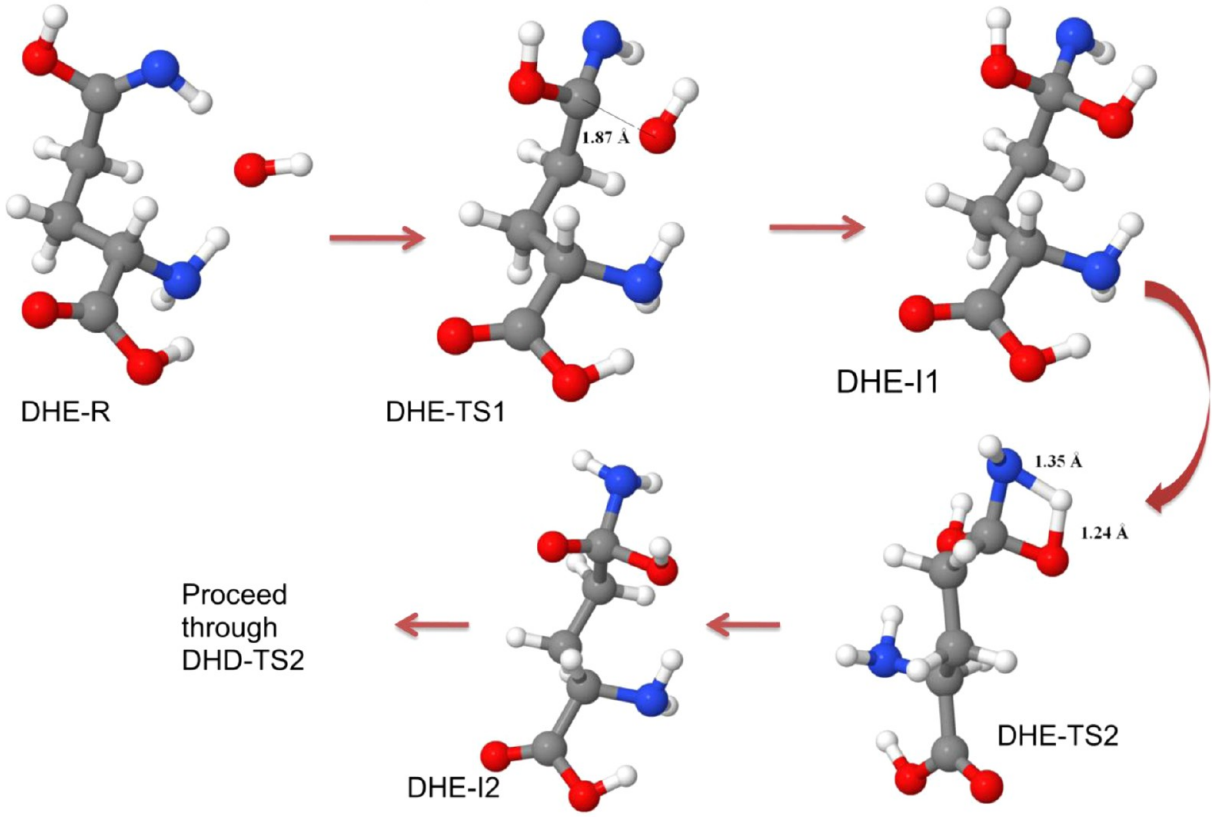

Figure 11. Pathway DHE: Direct hydrolysis of glutamine with hydroxide through a three-step mechanism, where optimized structures are generated at B3LYP/6-31+G(d,p).

31G(d), B3LYP/6-31+G(d,p), and G3MP2B3. The G3MP2B3 barrier, 197 kJ/mol, is in excellent agreement with the barrier calculated at B3LYP/6-31G(d) and B3LYP/6-31+G(d,p), differing by only 2 kJ/mol. The second step, which is rate-determining, involves a 1,3-proton transfer and elimination of NH_3. The overall barrier is 204, 215, and 204 kJ/mol at B3LYP/6-31G(d), B3LYP/6-31+G(d,p), and G3MP2B3, respectively, presented in Table 3 and Figure S11 (Supporting Information).

For the first step, PCM lowers the gas phase barrier by 4 kJ/mol, whereas SMD lowers the barrier by 6 kJ/mol, as depicted in Figure S12 (Supporting Information). For the second step, SMD lowers DHB-TS2 by 20 kJ/mol, whereas PCM decreases it by only 11 kJ/mol.

4.3. Pathway DHC: Mechanistic and Energetic Details of Direct Hydrolysis with Water. Deamidation of the glutamine tautomer with water is also investigated. In the first step, one proton transfers from the water to the ═NH, while the oxygen of the water molecule approaches the electron-deficient carbonyl carbon (see Figure S13, Supporting Information). In DHC-TS1, the O—H bond distance is 1.87 Å and the corresponding N—H bond distance is 1.05 Å, which indicates an almost complete proton transfer. The C—O bond distance (2.43 Å) is quite long compared to 1.99 and 2.08 Å in DHA-TS1 and DHB-TS1, respectively. IRC calculations on DHC-TS1 lead to the reactant DHC-R and the intermediate DHC-I1a. From DHC-I1a, the reaction follows pathway DHB through intermediate DHB-I1b. Except for SMD, the first step is rate-determining with an overall activation barrier of 180 kJ/mol at G3MP2B3.

4.4. Pathway DHD: Mechanistic and Energetic Details for Direct Hydrolysis with OH^-. The reaction of glutamine with OH^- produces a glutamate−NH_3 complex (DHD-P). It should be noted that a complex of glutamine with OH^- was only found with HF/6-31G(d). In DHD-TS1, the C−O and C−N distances are 1.79 and 1.47 Å, respectively, as shown in Figure S14 (Supporting Information). This mechanism is very similar to the deamination of cytosine and formamidine with hydroxide.[90,95] Forward and reverse IRC calculations show that in one direction DHD-TS1 connects with intermediate DHD-I1a and in the other direction it connects with a glutamine anion−H_2O complex (DHD-R) at all levels of theory and basis sets. IRC calculations connect DHD-TS2 to intermediate DHD-I1b. Conformers DHD-I1a and DHD-I1b are very similar, differing by no more than 19 kJ/mol in the gas phase and 9 kJ/mol in solution. In DHD-TS2, the C−N bond distance, 2.19 Å, is quite long and one proton from the C−OH is abstracted by NH_2^- (a very unstable anion) to form a glutamate−NH_3 complex, DHD-P (Figure S14, Supporting Information).

Large changes with solvent are observed for DHD-TS2, where the C−N bond distance (elimination of NH_3) increases from 2.19 to 2.23 and 2.21 Å with PCM and SMD, respectively. The N−H bond, involved in the 1,3-proton shift from the oxygen to the NH_2^-, also increases from 1.67 to 1.72 Å with PCM and decreases to 1.62 Å with SMD.

The overall barrier for the deamidation of glutamine with OH^- is predicted to be significantly higher than that for the deamidation with H_2O (pathway DHC), by 25 kJ/mol at G3MP2B3; see Table 3 and Figure S15 (Supporting Information). Inclusion of solvent water through PCM and

dx.doi.org/10.1021/jp4107266 | J. Phys. Chem. B 2014, 118, 2316−2330

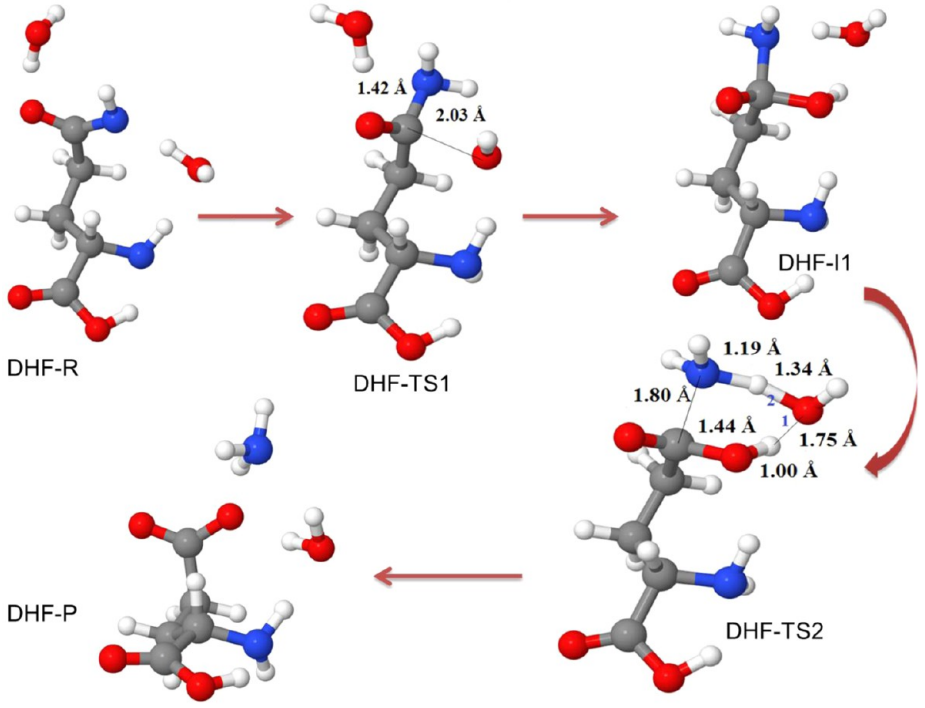

Figure 12. Pathway DHF: Direct hydrolysis of glutamine with OH^-/H_2O through a two-step mechanism, where optimized structures are generated at B3LYP/6-31+G(d,p).

SMD lowers both barrier heights for pathway DHD. With B3LYP/6-31+G(d,p), the gas phase barrier height for the first step is lowered by 38 kJ/mol with PCM and 25 kJ/mol with SMD. Solvent stabilizes both intermediates, DHD-I1a by 46 kJ/mol and DHD-I1b by no more than 58 kJ/mol with PCM and SMD, shown in Figure S16 (Supporting Information) and Table 3. The intermediate is now lower than the first transition state by 5 and 18 kJ/mol with PCM and SMD, respectively, compared to only 3 kJ/mol in the gas phase. The gas phase barrier height for the second step is lowered by 42 and 14 kJ/mol with PCM and SMD, respectively.

4.5. Pathway DHE: Mechanistic and Energetic Details for Direct Hydrolysis with OH^-. Pathway DHE has features similar to pathway DHD. In this case, the reactant is a complex of glutamine and hydroxide ion (GDE-R). In the first step, DHE-TS1, OH^- attacks the carbonyl carbon where the O—C bond distance is 1.87 Å (see Figure 11). In the second step, DHE-TS2, one proton transfers from oxygen to the ═NH to form intermediate DHE-I2a. The third step of this pathway is the same as the second step of pathway DHD, where a 1,3-proton shift from the oxygen to the nitrogen yields a glutamate—NH_3 complex. For pathway DHE, the second step is rate-determining with an overall barrier at G3MP2B3 of 135 kJ/mol compare to 205 kJ/mol for DHD.

4.6. Pathway DHF: Mechanistic and Energetic Details for Direct Hydrolysis with OH^-/H_2O. The direct hydrolysis of glutamine with OH^-/H_2O (pathway DHF) has the lowest overall barrier in comparison with all other pathways, except for G3MP3B3 where the lowest overall barrier is for pathway DHE. As shown in Figure 12, in the first step, the deprotonated glutamine—$2H_2O$ complex, DHF-R, undergoes nucleophilic attack by one of the water molecules at the carbonyl carbon, where the O—C bond distance is 2.03 Å (DHF-TS1), which is slightly longer compared to the O—C bond (1.79 Å) in DHD-TS1. The C—N bond distance is 1.42 Å, which is slightly shorter than the C—N bond (1.47 Å) in DHD-TS1. The second water molecule does not participate in the reaction but stabilizes the structures. IRC calculations on DHF-TS1 lead to an intermediate DHF-I1a and to the reactant, a complex of deprotonated glutamine with two water molecules (DHF-R). The second step is a water-mediated 1,3-proton shift also seen in the deamination of cytosine, guanine, and adenine with OH^-/H_2O.[90,94] In DHF-TS2, one proton from the OH group transfers through the water molecule to the nitrogen, shown in Figure 12, where the C—N bond length is 1.80 Å. IRC calculations on transition state DHF-TS2 lead to a product, $Glu^-\cdots NH_3\cdots H_2O$ complex and to intermediate DHF-I1b.

The structure of both transition states changes significantly with inclusion of implicit solvent water, especially DHF-TS2. In the gas phase, the C—N bond of DHF-TS2 decreases from 1.80 to 1.64 and 1.56 Å with PCM and SMD, respectively. The gas phase N—H bond length slightly decreased from 1.19 to 1.16 Å with SMD; however, it slightly increased to 1.33 Å with PCM. Both O—H bonds, denoted by 1 and 2 in Figure 12, also change significantly. The O—H(1) bond distance of the gas phase, PCM, and SMD is 1.75, 1.77, and 1.94 Å, whereas the O—H(2) bond, which transfers a proton from the oxygen to the nitrogen, is 1.34, 1.44, and 1.38 Å, respectively.

The second step is rate-determining with an overall barrier of 132, 146, and 143 kJ/mol at B3LYP/6-31G(d), B3LYP/6-31+G(d,p), and G3MP2B3, respectively, as depicted in Figure 13. As expected, on the basis of our previous work,[90,94] the water-mediated transition state, TS2, significantly lowers the overall barrier compared to pathways DHB, DHC, and DHD, although it is slightly higher (8 kJ/mol) compared to pathway DHE. For the rate-determining step of DHF, PCM lowers the barrier by 70 kJ/mol, whereas SMD lowers it by 71 kJ/mol (see Figure 14).

4.7. Comparison of Direct Hydrolysis Pathways. Enthalpies of activation and Gibbs energies of activation for

dx.doi.org/10.1021/jp4107266 | J. Phys. Chem. B 2014, 118, 2316−2330

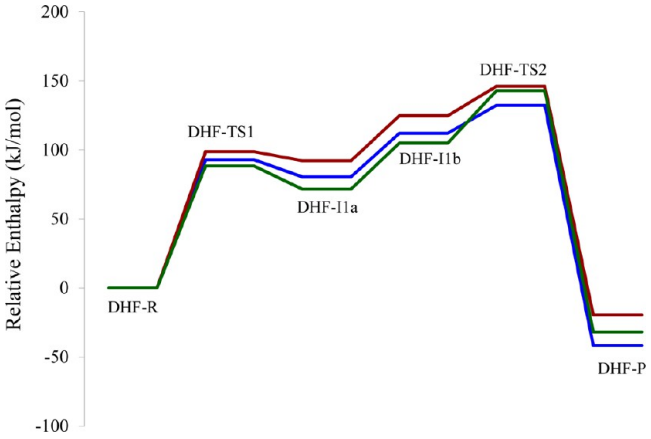

Figure 13. Pathway DHF: Gas phase relative enthalpies (kJ/mol) at B3LYP/6-31G(d) (blue), B3LYP/6-31+G(d) (red) and G3MP2B3 (green).

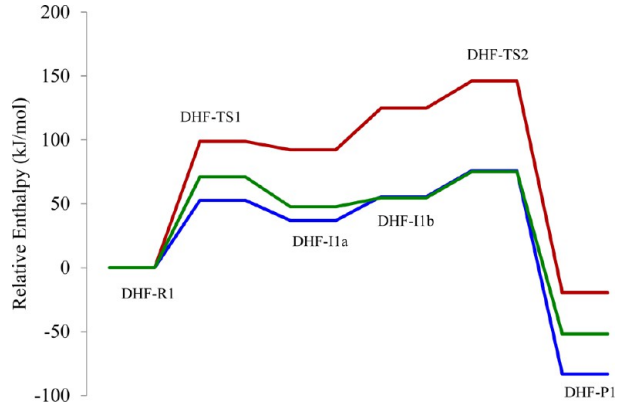

Figure 14. Pathway DHF: Relative enthalpies (kJ/mol) in the gas phase (red) and in the solvent phase with SMD (green) and PCM (blue) using B3LYP/6-31+G(d,p).

all pathways in direct hydrolysis are summarized in Table 3. In the gas phase, pathway DHA, the single-step concerted mechanism, has a barrier of 187 kJ/mol and the two-step mechanism, DHB, has an overall barrier of 204 kJ/mol at G3MP2B3. SMD lowers the DHA barrier from 180 to 171 kJ/mol at B3LYP/6-31+G(d,p). The overall reaction of Gln + H_2O → Glu + NH_3 is only slightly endothermic. On the other hand, hydrolysis of the Gln tautomer is exothermic and exergonic at all levels of theory except with SMD.

The calculated barriers of the deamidation with OH^- and OH^-/H_2O (pathways DHE and DHF) are noticeably lower than the deamidation with H_2O. In the gas phase, pathway DHE, the two-step concerted mechanism, has the lowest overall barrier of 135 kJ/mol at G3MP2B3. PCM and SMD, however, increase this overall barrier to 144 and 136 kJ/mol, respectively, at B3LYP/6-31+G(d,p). The lowest barrier is for pathway DHF, with a gas phase barrier of 143 kJ/mol at G3MP2B3 and 75 kJ/mol with SMD at the B3LYP/6-31+G(d,p) level of theory. The overall reaction of Gln + OH^- → Glu^- + NH_3 is highly exothermic and exergonic due to the high stability of Glu^- compared to OH^-; see Table 3.

5. COMPARATIVE ANALYSIS

It is worthwhile to compare the energetics of glutamine deamidation with other systems, including deamidation of asparaginyl residues and deamination of cytosine, adenine, and guanine, since they share some similar mechanistic features. The lowest calculated activation barrier for the deamidation of asparagine (Asn) residue through a cyclic succinimide mediated pathway with two water molecules is 166 kJ/mol, which is lower than the barrier for the direct hydrolysis (180 kJ/mol) at B3LYP/6-31+G(d,p).[69] However, the experimental barrier, 155 ± 0.08 kJ/mol, for the deamidation of sodium-bound asparagine (Na^+Asn) is in good agreement with the theoretical barrier, 163−168 kJ/mol, computed at B3LYP, B3P86, and MP2 theories using the 6-311+G(2d,2p) basis set.[56] These experimental and theoretical results for sodium-bound asparagine deamidation are lower than the theoretical barrier for asparaginyl residues. The calculated barrier height, 115 kJ/mol, for the deamination of cytosine with OH^-/H_2O is in good agreement with the experimental barrier 117 kJ/mol.[91,101] Platinum catalyst (Pt) significantly reduced the barrier height to 99 kJ/mol for the deamination of cytosine.[97] The activation barriers for the deamination of guanine (144 kJ/mol, at G3MP2)[92] and adenine (98 kJ/mol[99] and 139 kJ/mol[94]) are comparable with the gas phase direct hydrolysis result for glutamine (135 kJ/mol). The lowest gas phase barrier (133 kJ/mol) for the deamination of methyl cytosine is decreased to 95 kJ/mol in solution with Monte Carlo simulation using the B3LYP/6-311G(d,p) level of theory,[100] which is 20 kJ/mol higher than the barrier obtained for pathway DHF in solution.

6. CONCLUDING REMARKS

In this study, glutamine deamidation and hydrolysis of oxoproline are investigated computationally for the cyclic and direct approaches along with neutral and basic media, and compared with other deamidation systems. We observe that direct hydrolysis mechanisms with OH^- and OH^-/H_2O are energetically more favored compared to all other pathways. These pathways, DHE and DHF, show the lowest activation barrier, 135 and 143 kJ/mol, respectively, in the gas phase with the G3MP2B3 level of theory. Incorporating implicit solvent does not decrease the barrier height of pathway DHE. The addition of one water molecule, pathway DHF, significantly lowers the barrier height with both PCM and SMD solvation models. With only a few exceptions, for nearly all pathways, the SMD solvation model shows a lower activation barrier than that for PCM. The lowest activation barrier, 75 kJ/mol, is found for pathway DHF with SMD at B3LYP/6-31+G(d,p). The performance of the SMD solvation model can be explained by the parametrization of CDS terms (cavitations, dispersion, and solvent structure effect), which can successfully treat the polarization and non-electrostatic effects in shorter range, including both hydrogen bonding and exchange repulsion effects. These terms in SMD contribute in lowering the activation barrier for almost all pathways. The presence of an additional water molecule in pathway DHF significantly lowers the barrier height for the glutamine deamidation by stabilizing the transition state structure through a network of hydrogen bonds and transferring the proton through the water mediated channel.

■ ASSOCIATED CONTENT

Supporting Information

Figures S1−S16 (PES of different pathways for deamidation of glutamine) and full geometries and energies of all structures for all pathways investigated at all levels of theory discussed in the

dx.doi.org/10.1021/jp4107266 | J. Phys. Chem. B 2014, 118, 2316−2330

present paper. This material is available free of charge via the Internet at http://pubs.acs.org.

AUTHOR INFORMATION

Corresponding Authors

*E-mail: almatarneh@yahoo.com. Phone: +1709-864-8609.
*E-mail: rpoirier@mun.ca. Phone: +1709-864-8609.

Notes

The authors declare no competing financial interest.

ACKNOWLEDGMENTS

We gratefully acknowledge the Atlantic Computational Excellence Network (ACEnet) for computer time and the Natural Sciences and Engineering Council of Canada (NSERC) for financial support.

REFERENCES

(1) Antonio, J.; Street, C. *Can. J. Appl. Physiol.* **1999**, *24*, 1−14.
(2) Carvalho-Peixoto, J.; Alves, R. C.; Cameron, L. *Appl. Physiol., Nutr., Metab.* **2007**, *32*, 1186−1190.
(3) Castell, L.; Poortmans, J.; Newsholme, E. *Eur. J. Appl. Physiol. Occup. Physiol.* **1996**, *73*, 488−490.
(4) Gleeson, M. *J. Nutr.* **2008**, *138*, 2045S−2049S.
(5) Graham, T. E. *FASEB J.* **1998**, *12*, 5470.
(6) Rohde, T.; Krzywkowski, K.; Pedersen, B. *Exercise Immunol. Rev.* **1998**, *4*, 49−63.
(7) Albrecht, J.; Norenberg, M. D. *Hepatology* **2006**, *44*, 788−794.
(8) Albrecht, J.; Sonnewald, U.; Waagepetersen, H. S.; Schousboe, A. *Front. Biosci.* **2007**, *12*, 332−343.
(9) Albrecht, J.; Dolinska, M. *J. Neurosci. Res.* **2001**, *65*, 1−5.
(10) Albrecht, J.; Zielinska, M.; Norenberg, M. D. *Biochem. Pharmacol.* **2010**, *80*, 1303−1308.
(11) Sanyal, A. J.; Bosch, J.; Blei, A.; Arroyo, V. *Gastroenterology* **2008**, *134*, 1715−1728.
(12) Newsholme, P.; Lima, M. M. R.; Porcopio, J.; Pithon-Curi, T. C.; Doi, S. Q.; Bazotte, R. B.; Curi, R. *Braz. J. Med. Biol. Res.* **2003**, *36*, 153−163.
(13) Curi, R.; Lagranha, C.; Doi, S.; Sellitti, D.; Procopio, J.; Pithon-Curi, T.; Corless, M.; Newsholme, P. *J. Cell. Physiol.* **2005**, *204*, 392−401.
(14) Young, V.; Ajami, A. *J. Nutr.* **2001**, *131*, 2449S−2459S.
(15) Aledo, J. *Bioessays* **2004**, *26*, 778−785.
(16) Curi, R.; Newsholme, P.; Procopio, J.; Lagranha, C.; Gorjao, R.; Pithon-Curi, T. C. *Front. Biosci.* **2007**, *12*, 344−357.
(17) Daikhin, Y.; Yudkoff, M. *J. Nutr.* **2000**, *130*, 1026S−1031S.
(18) Brosnan, J. T. *J. Nutr.* **2003**, *133*, 2068S−2072S.
(19) Lee, W. J.; Hawkins, R. A.; Vina, J. R.; Peterson, D. R. *Am. J. Physiol.: Cell Physiol.* **1998**, *274*, C1101−C1107.
(20) Yuneva, M.; Zamboni, N.; Oefner, P.; Sachidanandam, R.; Lazebnik, Y. *J. Cell Biol.* **2007**, *178*, 93−105.
(21) Bode, B. P. *J. Nutr.* **2001**, *131*, 2475S−2485S.
(22) Bak, L. K.; Schousboe, A.; Waagepetersen, H. S. Glutamate and glutamine in brain disorders. In *Neurochemical mechanism in disease, Advanced in Neurobiology*; Blass, J. P., Ed.; Springer Science: New York, 2011.
(23) Bak, L. K.; Schousboe, A.; Waagepetersen, H. S. *J. Neurochem.* **2006**, *98*, 641−653.
(24) Waagepetersen, H. S., Schousboe, A. Sonnewald, U. Glutamate, glutamine and gaba: metabolic aspects. In *Handbook of neurochemistry and molecular neurobiology*; Oja, S. S., Schousboe, A, Saransaari, P, Eds.; Springer-Verlag: Heidelberg, Germany, 2007.
(25) Waagepetersen, H. S.; Sonnewald, U.; Schousboe, A. *Neuroscientist* **2003**, *9*, 398−403.
(26) Braissant, O. *Mol. Genet. Metab.* **2010**, *100*, S3−S12.
(27) Kerbs, H. A. *Biochem. J.* **1936**, *29*, 1951−1969.
(28) Weil-Malherbe, H. *Physiol. Rev.* **1950**, *30*, 549−568.
(29) Warren, K. S.; Schenker, S. *J. Lab. Clin. Med.* **1964**, *64*, 442−449.
(30) Norenberg, M. D.; Hernandez, A. M. *Brain Res.* **1979**, *161*, 303−310.
(31) Jessy, J.; DeJoseph, M. R.; Hawkins, R. A. *Biochem. J.* **1991**, *277*, 693−696.
(32) Hawkins, R. A.; Jessy, J. *Biochem. J.* **1991**, *277*, 697−703.
(33) Lemberg, A.; Fernandez, M. A. *Ann. Hepatol.* **2009**, *8*, 95−102.
(34) Norenberg, M. D.; Jayakumar, A. R.; Rao, K. V. R. *Metab. Brain Dis.* **2004**, *19*, 313−329.
(35) Norenberg, M. D.; Rao, K. V.; Jayakumar, A. R. *Metab. Brain Dis.* **2005**, *20*, 303−318.
(36) Norenberg, M. D.; Rao, K. V. R.; Jayakumar, A. R. *J. Bioenerg. Biomembr.* **2004**, *36*, 303−307.
(37) Rao, K. V. R.; Jayakumar, A. R.; Norenberg, M. D. *Neurochem. Int.* **2005**, *47*, 31−38.
(38) Dams, K.; Meersseman, W.; Wilmer, A. Hyperammonemia in the Adult Critical Care Setting. *Yearbook of Intensive Care and Emergency Medicine 2008*; Springer-Verlag: Berlin, 2008; section XII, pp 481−490.
(39) Albrecht, J.; Jones, E. A. *J. Neurol. Sci.* **1999**, *170*, 138−146.
(40) Albrecht, J.; Wegrzynowicz, M. *Metab. Brain Dis.* **2005**, *20*, 253−263.
(41) Cohn, R. M.; Roth, K. S. *Clin. Pediatr.* **2004**, *43*, 683−689.
(42) Pucher, G. W.; Vicary, H. B. *Ind. Eng. Chem. Anal. Ed.* **1940**, *12*, 27−29.
(43) Hamilton, P. B. *J. Biol. Chem.* **1945**, *158*, 375−395.
(44) Talley, E. A.; Fitzpatrick, T. J.; Porter, W. L. *J. Am. Chem. Soc.* **1956**, *78*, 5836−5837.
(45) Wright, H. *Crit. Rev. Biochem. Mol. Biol.* **1991**, *26*, 1−52.
(46) Capasso, S.; Mazzarella, L.; Sica, F.; Zagari, A. *J. Chem. Soc., Chem. Commun.* **1991**, 1667−1668.
(47) Robinson, N.; Robinson, A. *Proc. Natl. Acad. Sci. U.S.A.* **2001**, *98*, 12409−12413.
(48) Robinson, N.; Robinson, Z.; Robinson, B.; Robinson, A.; Robinson, J.; Robinson, M.; Robinson, A. *J. Pept. Res.* **2004**, *63*, 426−436.
(49) Robinson, N. E.; Robinson, A. B. *Biopolymers* **2008**, *90*, 297−306.
(50) Rivers, J.; McDonald, L.; Edwards, I. J.; Beynon, R. J. *J. Proteome Res.* **2008**, *7*, 921−927.
(51) Robinson, A.; Robinson, L. *Proc. Natl. Acad. Sci. U.S.A.* **1991**, *88*, 8880−8884.
(52) Robinson, A.; Scotchle, J. W.; Mckerrow, J. *J. Am. Chem. Soc.* **1973**, *95*, 8156−8160.
(53) Geiger, T.; Clarke, S. *J. Biol. Chem.* **1987**, *262*, 785−794.
(54) Robinson, N.; Robinson, A. *Mech. Ageing Dev.* **2004**, *125*, 259−267.
(55) Seo, J.; Lee, K. *J. Biochem. Mol. Biol.* **2004**, *37*, 35−44.
(56) Heaton, A. L.; Armentrout, P. B. *J. Am. Chem. Soc.* **2008**, *130*, 10227−10232.
(57) Baynes, J. *Biogerontology* **2000**, *1*, 235−246.
(58) Hipkiss, A. *Biogerontology* **2001**, *2*, 173−178.
(59) Robinson, A. *Mech. Ageing Dev.* **1979**, *9*, 225−236.
(60) Robinson, A.; Willoughby, R.; Robinson, L. *Exp. Gerontol.* **1976**, *11*, 113−120.
(61) Weintraub, S.; Manson, S. *Mech. Ageing Dev.* **2004**, *125*, 255−257.
(62) Wilmarth, P. A.; Tanner, S.; Dasari, S.; Nagalla, S. R.; Riviere, M. A.; Bafna, V.; Pevzner, P. A.; David, L. L. *J. Proteome Res.* **2006**, *5*, 2554−2566.
(63) Takemoto, L.; Emmons, T. *Curr. Eye Res.* **1991**, *10*, 865−869.
(64) Groenen, P.; Vandongen, M.; Voorter, C.; Bloemendal, H.; Dejong, W. *FEBS Lett.* **1993**, *322*, 69−72.
(65) Hains, P. G.; Truscott, R. J. W. *Invest. Ophthalmol. Vis. Sci.* **2010**, *51*, 3107−3114.
(66) Robinson, N.; Robinson, A. *Proc. Natl. Acad. Sci. U.S.A.* **2001**, *98*, 944−949.

(67) Robinson, N. E.; Robinson, A. B. *Molecular Clocks: Deamidation of Asparaginyl and Glutaminyl Residues in Peptides and Proteins*; Althouse Press: Cave Junction, OR, 2004.
(68) Liu, H.; Gaza−Bulsecon, G.; Chumsae, C. *Rapid Commun. Mass Spectrom.* **2008**, *22*, 4081−4088.
(69) Catak, S.; Monard, G.; Aviyente, V.; Ruiz-Lopez, M. F. *J. Phys. Chem. A* **2009**, *113*, 1111−1120.
(70) Scotchle, J. W.; Robinson, A. *Anal. Biochem.* **1974**, *59*, 319−322.
(71) Capasso, S.; Mazzarella, L.; Sica, F.; Zagari, A.; Salvadori, S. *J. Chem. Soc., Perkin Trans. 2* **1993**, 679−682.
(72) Capasso, S. *J. Pept. Res.* **2000**, *55*, 224−229.
(73) Konuklar, F.; Aviyente, V.; Sen, T.; Bahar, I. *J. Mol. Model.* **2001**, *7*, 147−160.
(74) Konuklar, F.; Aviyente, V.; Lopez, M. *J. Phys. Chem. A* **2002**, *106*, 11205−11214.
(75) Catak, S.; Monard, G.; Aviyente, V.; Ruiz-Lopez, M. F. *J. Phys. Chem. A* **2006**, *110*, 8354−8365.
(76) Catak, S.; Monard, G.; Aviyente, V.; Ruiz-Lopez, M. F. *J. Phys. Chem. A* **2008**, *112*, 8752−8761.
(77) Peters, B.; Trout, B. *Biochemistry* **2006**, *45*, 5384−5392.
(78) Kaliman, I.; Nemukhin, A.; Varfolomeev, S. *J. Chem. Theory Comput.* **2010**, *6*, 184−189.
(79) Patel, K.; Borchardt, R. T. *Pharm. Res.* **1990**, *7*, 703−711.
(80) Frisch, M. J.; et al. *Gaussian 09*, revision A.1; Gaussian, Inc.: Wallingford, CT, 2009.
(81) Onsager, L. *J. Am. Chem. Soc.* **1936**, *58*, 1486−1493.
(82) Cramer, C. J.; Truhlar, D. G. *Chem. Rev.* **1999**, *99*, 2161−2200.
(83) Rivail, L.; Rinaldi, D. *Theor. Chim. Acta* **1973**, *32*, 57−70.
(84) Tomasi, J.; Persico, M. *Chem. Rev.* **1994**, *94*, 2027−2094.
(85) Rivail, J. L.; Rinaldi, D.; Luiz−Lopez, M. F. Liquid State Quantum Chemistry. In *Computational Chemistry: Review of Current Trends*; Lecszynski, J., Ed.; World Scientific: Singapore, 1995.
(86) Cossi, M.; Rega, N.; Scalmani, G.; Barone, V. *J. Chem. Phys.* **2001**, *114*, 5691−5701.
(87) Miertu, S.; Scrocco, E.; Tomasi, J. *Chem. Phys.* **1981**, *55*, 117−129.
(88) Marenich, A. V.; Cramer, C. J.; Truhlar, D. G. *J. Phys. Chem. B* **2009**, *113*, 6378−6396.
(89) Halim, M. A.; Shaw, D. M.; Poirier, R. A. *J. Mol. Struct.: THEOCHEM* **2010**, *960*, 63−72.
(90) Almatarneh, M.; Flinn, C.; Poirier, R.; Sokalski, W. *J. Phys. Chem. A* **2006**, *110*, 8227−8234.
(91) Almatarneh, M. H.; Flinn, C. G.; Poirier, R. A. *J. Chem. Inf. Model.* **2008**, *48*, 831−843.
(92) Uddin, K. M.; Almatarneh, M. H.; Shaw, D. M.; Poirier, R. A. *J. Phys. Chem. A* **2011**, *115*, 2065−2076.
(93) Uddin, K. M.; Poirier, R. A. *J. Phys. Chem. B* **2011**, *115*, 9151−9159.
(94) Alrawashdeh, A.; Almatarneh, M. H.; Poirier, R. A. *Can. J. Chem.* **2013**, *91* (7), 518−526.
(95) Flinn, C.; Poirier, R. A.; Sokalski, W. A. *J. Phys. Chem. A* **2003**, *107*, 11174−11181.
(96) Zhang, A.; Yang, B.; Li, Z. *J. Mol. Struct.: THEOCHEM* **2007**, *819*, 95−101.
(97) Sponer, J.; Miguel, P.; Rodriguez-Santiago, L.; Erxleben, A.; Krumm, M.; Sodupe, M.; Sponer, J.; Lippert, B. *Angew. Chem., Int. Ed.* **2004**, *43*, 5396−5399.
(98) Wang, H.; Meng, F. *Theor. Chem. Acc.* **2010**, *127*, 561−571.
(99) Zheng, H.; Meng, F. *Struct. Chem.* **2009**, *20*, 943−949.
(100) Chen, Z. Q.; Zhang, C. H.; Kim, C. K.; Xue, Y. *Phys. Chem. Chem. Phys.* **2011**, *13*, 6471−6483.
(101) Frederico, L.; Kunkel, T.; Shaw, B. *Biochemistry* **1993**, *32*, 6523−6530.